

Electrodeposition of crystalline Co_3O_4 – a catalyst for the oxygen evolution reaction

Jakub A. Koza, Zhen He, Andrew S. Miller, and Jay A. Switzer*

Department of Chemistry and Graduate Center for Materials Research, Missouri University of Science and Technology, Rolla, Missouri 65409-1170, USA

*To whom correspondence should be addressed. E-mail: jswitzer@mst.edu

This file includes:

Figures S1 to S6

1. Electro-oxidation of the ligand (tartrate) – Cyclic voltammogram in the electrolyte without Co^{2+} ions

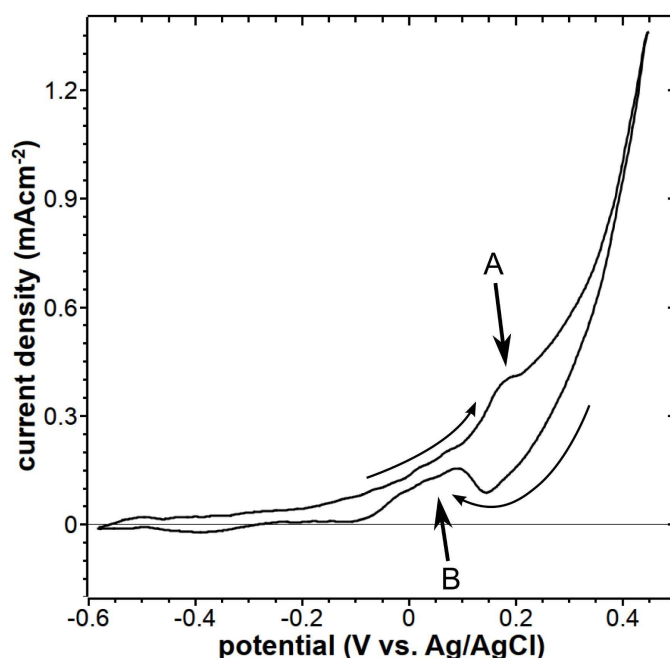


Figure S1. Cyclic voltammogram of 6 mM tartrate in 2 M NaOH electrolyte. Au electrode, 103 °C (reflux), 50 mV s⁻¹.

Figure S1 show a cyclic voltammogram (CV) measured in 6 mM tartrate in 2 M NaOH electrolyte at reflux. Two peaks in the CV can be observed, one in the forward scan with a maximum at a potential of about 175 mV (A) and a second one in the backward scan with a maximum at a potential of about 100 mV (B). Both of the peaks have positive charge. This is a characteristic feature for the tartaric acid electro-oxidation in alkaline electrolyte.^{S1,S2,S3}

(S1) Bohannan, E. W.; Kothari, H. M.; Nicic, I. M.; Switzer, J. A. *J. Am. Chem. Soc.* **2004**, 126, 488.

(S2) Switzer, J. A. *Interface* **2004**, winter, 34.

(S3) Sarkar, S. K.; Burla, N.; Bohannan, E. W.; Switzer, J. A. *J. Am. Chem. Soc.* **2007**, 129, 8972.

2. Experimental conditions, XRD pattern, and Raman spectrum of the Co_3O_4 film deposited on $p^+\text{-Si}(110)$

The experimental conditions were the same as for deposition on a SS substrate unless otherwise mentioned. The film was deposited from a refluxing electrolyte at 400 mV vs. Ag/AgCl for 100 s. The substrate was H-terminated, $p^+\text{-Si}(110)$ (boron doped, 0.005 Ω cm). The H-terminated substrate was prepared by immersing it in 5 % HF for one minute followed by immersion in hot HPLC H_2O for about 20 min. Finally, just prior to depositing, the substrate was immersed in 5 % HF for 10 s and rinsed with HPLC H_2O .

In the case of the deposition on Si it was not possible to use galvanostatic conditions as on other substrates. This is because at the current densities, which resulted in good quality deposits on the SS, the potentials at the Si substrate were in the range of the Si oxidation and no film deposition was noticed.

Instead, potentiostatic conditions were chosen. Figure S2a shows the XRD pattern of the Co_3O_4 film deposited on the Si(110) substrate at 400 mV. Although, the pattern is noisy, due to the thickness of the film and the grazing incident geometry employed, the peaks of the Co_3O_4 are revealed. The spinel Co_3O_4 structure formation on Si substrate was further confirmed by Raman spectroscopy investigations. Raman spectroscopy measurements were carried out using a Horiba Jobin-Yvon LabRam Aramis Microscope with a HeNe laser ($\lambda=633$ nm) as the excitation source with an incident power of about 0.5 mW to minimize sample heating. Figure S2b shows the Raman spectrum of the film deposited on the Si substrate. The measured spectrum is in a very good agreement with that of Co_3O_4 ,^{S4,S5} the peak at about 520 cm^{-1} originates from the Si substrate.

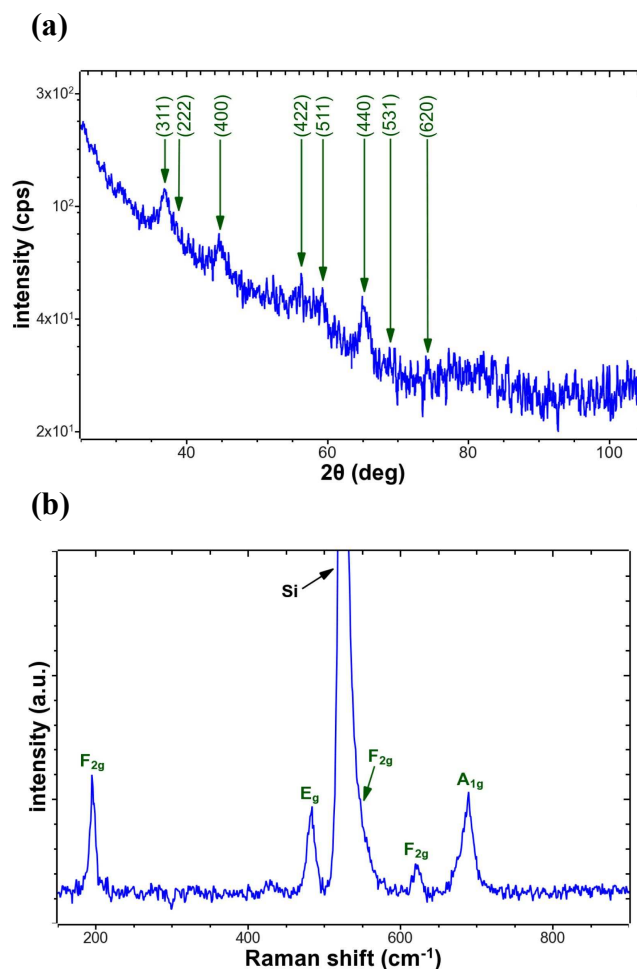


Figure S2. (a) XRD pattern (grazing incidence geometry) of Co_3O_4 film deposited on H-Si(110) substrate with indicated indices (JCPDS#42-1467), (b) Raman spectrum of Co_3O_4 film deposited on H-Si(110) substrate with indicated Raman-active phonon modes.^{S4,S5} Film deposited at 400 mV vs. Ag/AgCl for 100 s at 103°C (reflux).

(S4) Hadjiev, V. G.; Iliev, M. N.; Vergilov, I. V. *J. Phys. C* **1988**, *21*, L199.

(S5) Wang, G.; Shen, X.; Horvat, J.; Wang, B.; Liu, H.; Wexler, D.; Yao, J. *J. Phys. Chem. C* **2009**, *113*, 4357.

3. Determination of the in-plane orientation of Co_3O_4 film electrodeposited on $\text{Au}(100)$ substrate

The (311) pole figure for Co_3O_4 on $\text{Au}(100)$ is shown in the main text (Figure 5b). The pole figure was acquired by setting the 2θ angle to 36.853° and azimuthally rotating the sample from 0 to 360° (Φ angle), at tilt angles (ψ) from 0 to 90° . The peaks are observed in the pole figure aligned in rings, 12 equally spaced peaks at each ring, at ψ angles of 29.5° , 58.5° , and 80° . The low intensity peak in the center of the pole figure corresponds to the (311) plane, which was also observed at very low intensity in the XRD pattern (Figure 5a in the main text). The in-plane orientation of the film could be resolved by comparing the measured pole figure with the corresponding stereographic projection generated using CaRIne 3.1 software. A single domain stereographic projection is shown in Figure S3a. By comparing the projection with the measured pole figure it is apparent that all the observed peaks match the interplanar angles between $\{311\}$ and $\{111\}$. However, the single domain projection does not predict 12 peaks at each of the rings but only 3 peaks at $\psi=29.5^\circ$, 6 peaks at $\psi=58.5^\circ$, and 3 peaks at $\psi=80^\circ$. This is because the $\text{Au}(100)$ plane has 4-fold symmetry and the measured pole figure represents 4 domains of $\text{Co}_3\text{O}_4(111)$ rotated by 90° . This is clearly visible in the stereographic projection shown in Figure S3b, where 4 domains are rotated by 90° . The intensity of peaks at each of the rings is predicted to be equal, as observed in the measured pole figure, because the peaks originating from different domains either do not overlap or overlap twice (at $\psi=58.5^\circ$).

The epitaxial relationship was determined with a help of the stereographic projections (Figure S3a,b) and comparing the azimuthal (Φ) scans of the Co_3O_4 film ($2\theta = 36.853^\circ$, $\psi = 29.5^\circ$) and the $\text{Au}(100)$ substrate ($2\theta = 64.7^\circ$, $\psi = 45^\circ$) (Figure S3c). Based on the azimuthal scans, it was found that the film is rotated in plane by 45° with respect to the substrate. Hence, considering the four domains, the epitaxial relationship is found to be $\text{Co}_3\text{O}_4(111)[11\ \bar{2}]\parallel\text{Au}(100)\langle 001\rangle$.

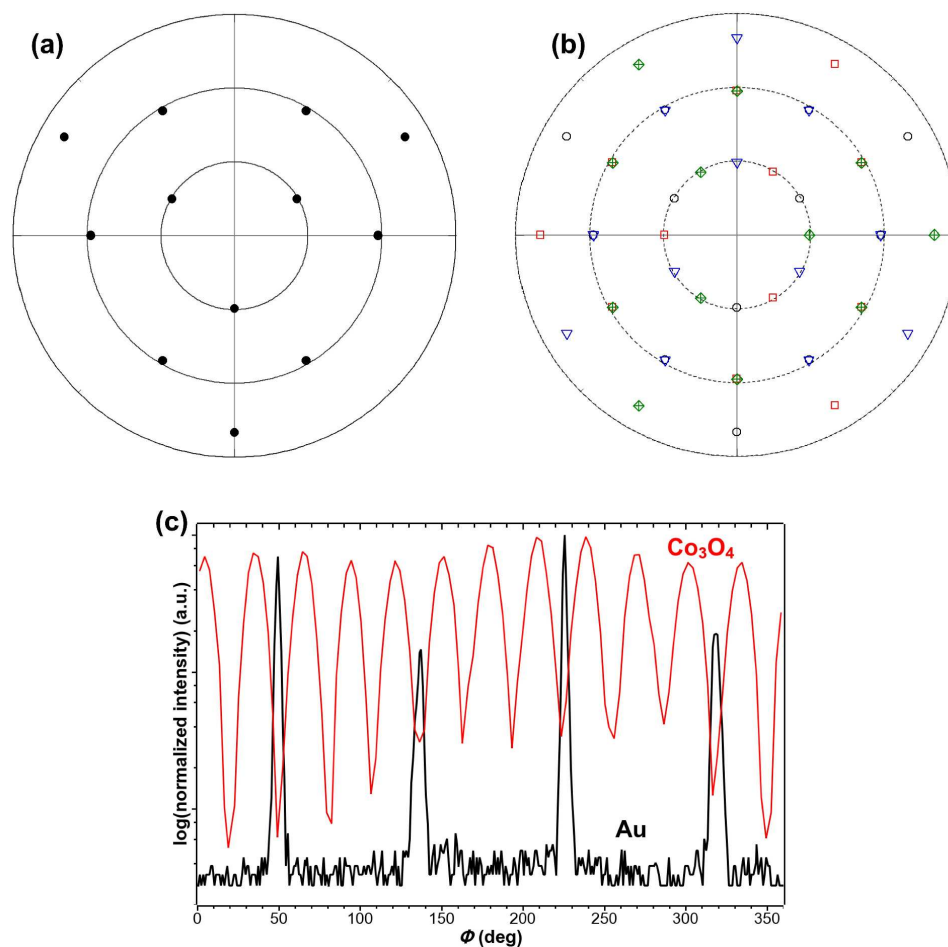


Figure S3. Stereographic projections of the (311) pole figures of $\text{Co}_3\text{O}_4(111)$: (a) single domain, and (b) four superposed domains, different shapes and colors stand for different domains rotated in-plane by 90° . (c) Experimentally observed azimuthal (Φ) scans of the Co_3O_4 film (red) and Au substrate (black). Au(100) substrate, 0.25 mA cm^{-2} , 0.9 C cm^{-2} , 103°C (reflux).

4. Scanning electron microscope (SEM) images of the Co_3O_4 films deposited on SS substrates

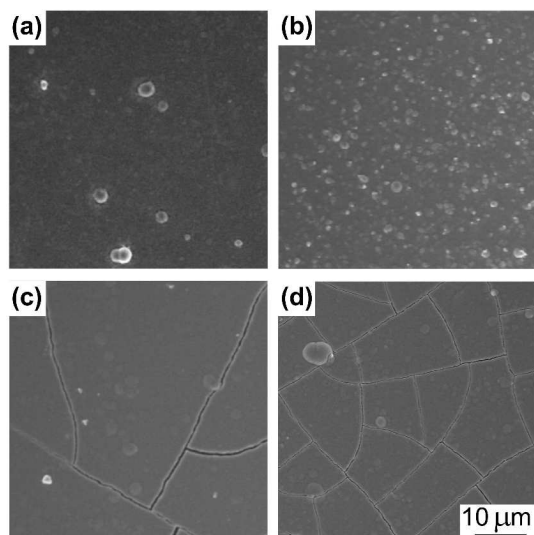


Figure S4. SEM images of the Co_3O_4 films deposited from a refluxing electrolyte at (a) 0.25 mA cm^{-2} , (b) 0.5 mA cm^{-2} , (c) 0.75 mA cm^{-2} , and (d) 1 mA cm^{-2} . SS substrate, 0.9 C cm^{-2} .

Figure S3 shows the SEM images of the Co_3O_4 films deposited at different current densities from a refluxing electrolyte. It can be seen that films deposited at current densities higher than 0.5 mA cm^{-2} show significant cracking.

5. LSVs of the Co_3O_4 films and substrates

Figure S5a shows the LSVs measured on a Co_3O_4 film as well as on the SS substrate in 1 M KOH at room temperature. The Co_3O_4 film is significantly more active than the substrate. The onset overpotential for oxygen evolution on Co_3O_4 appears at about 0.325 V, which is approximately 50 mV lower than on the SS substrate. Also the slope of the rising part of the curve (OER) is higher for the Co_3O_4 film compared to the SS substrate. Additionally, the LSVs measured on Co_3O_4 film deposited on Ti substrate together with the bare Ti substrate are shown in Figure S5b. From Figure S5b it is clear that the catalytic properties are related purely to the film, without any significant contribution of the substrate (Ti has negligible OER current in the studied potential range). A peak observed just prior to the onset of OER is consisted with the oxidation of Co^{3+} to Co^{4+} .^{S6,S7,S8}

(S6) Innocenzo G, C. *J. Electroanal. Chem.* **2002**, 520, 119.

(S7) Casella, I. G.; Di Fonzo, D. A. *Electrochim. Acta* **2011**, 56, 7536.

(S8) Singh, R. N.; Koenig, J. F.; Poillerat, G.; Chartier, P. *J. Electrochem. Soc.* **1990**, 137, 1408.

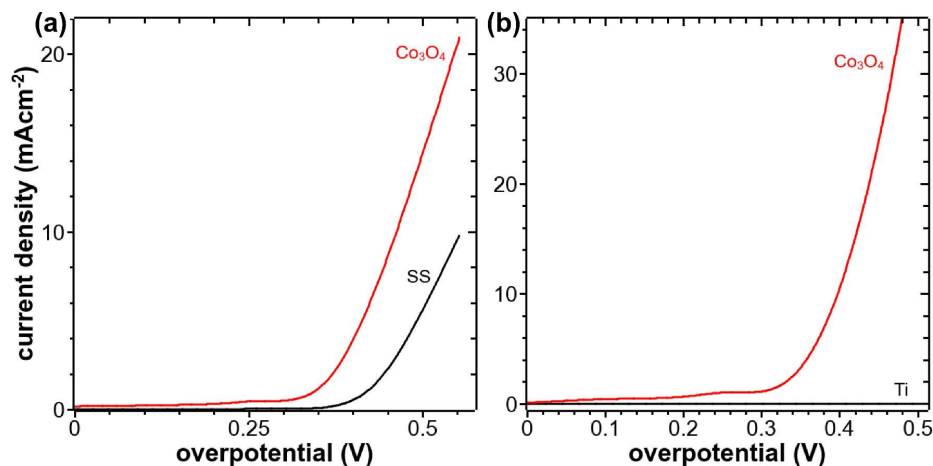


Figure S5. (a) LSV measured on the Co_3O_4 film (red) deposited on SS and the LSV of bare SS substrate (black). (b) LSV measured on the Co_3O_4 film (red) deposited on Ti and the LSV of bare Ti substrate (black). The films deposited at 0.25 mA cm^{-2} from refluxing electrolyte at constant charge density of 0.9 C cm^{-2} .

6. Tafel plots of Co_3O_4 film deposited on SS with and without the electrolyte IR correction

Figure S6 shows the steady state polarization curves measured on a crystalline Co_3O_4 film in 1 M KOH at room temperature. The red curve was not corrected for electrolyte IR drop. The blue curve was corrected for the electrolyte IR (this is the curve in the main paper). The resistance ($R = 1.3 \Omega$) was determined with electrochemical impedance spectroscopy (EIS). At low current densities the correction is insignificant and does not affect the Tafel slope (49 mV dec^{-1}). However, at high current densities (higher than about 10 mA cm^{-2}) the curves deviate.

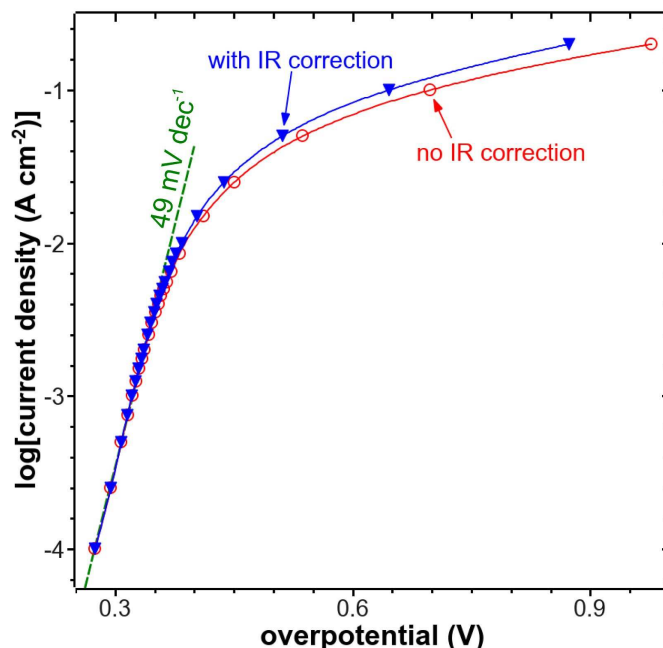


Figure S6. Steady state polarization curves of electrodeposited Co_3O_4 film without (red line and open circles) and with (blue line and triangles) the electrolyte IR correction. Co_3O_4 deposited at 0.25 mA cm^{-2} from a refluxing electrolyte on a SS substrate by passing a charge density of 0.9 C cm^{-2} . The overpotential was calculated with respect to the thermodynamic potential at pH of 14 of 0.401 V vs. NHE.